Processing and Application of Ceramics 12 [1] (2018) 45–55
https://doi.org/10.2298/PAC1801045Z

Effects of sintering temperature and holding time on the microstructure and electric properties of $Ba(Zr_{0.3}Ti_{0.7})O_3$ ceramics

Xiaoya Zhang[1], Gang Chen[1,2,*], Chunlin Fu[1], Wei Cai[1], Rongli Gao[1], Fengqi Wang[1]

[1]*School of Metallurgy and Materials Engineering, Chongqing University of Science and Technology, Chongqing, 401331, PR China*
[2]*Colleges of Materials Science and Engineering, Chongqing University, Chongqing, 400044, PR China*

Received 26 August 2017; Received in revised form 31 December 2017; Accepted 10 February 2018

Abstract

$Ba(Zr_{0.3}Ti_{0.7})O_3$ (BZT) ceramics was prepared by using conventional solid state reaction. The effects of sintering temperature and holding time on the crystal structure, surface morphology, dielectric, ferroelectric and piezoelectric properties of the BZT ceramics were systematically investigated. X-ray diffraction (XRD) results confirm single cubic perovskite phase in all the sintered samples. Microstructure analysis using scanning electron microscopy (SEM) reveals that the grain sizes increase with increasing the sintering temperature. Dielectric spectroscopy performed in the range of 20 Hz to 2 MHz at room temperature shows that the dielectric constant increases with the sintering temperature and the dielectric constant of the BZT ceramics sintered at 1400 °C for 8 h is around 11500. The ferroelectric hysteresis loops show that the coercive field decreases with the holding time, while the remnant polarization does not change obviously. The maximum strain is 0.023% for the sample sintered at 1400 °C for 4 h. It is found that the maximum value of the direct piezoelectric coefficient (d_{33}) of the BZT ceramics sintered at 1400 °C for 8 h measured at room temperature is 36.7 pC/N.

Keywords: *barium zirconate titanate, sintering temperature, holding time, electrical performance*

I. Introduction

Barium titanate ($BaTiO_3$, BTO), ferroelectric material with excellent dielectric, piezoelectric and ferroelectric properties, has been attracting increasing attention due to its widespread application in multilayer ceramic capacitor, thermistor, ferroelectric random access memory, resonator, temperature sensor, piezoelectric sensor, photoelectric device, actuator, etc. [1,2]. In order to further reduce the dielectric loss at low frequencies and increase the stability of the dielectric constant at bias voltages, Zr^{4+} was usually chosen as dopant to form barium zirconate titanate ($Ba(Zr_xTi_{1-x})O_3$, BZT) [3,4]. BZT is a potential candidate as lead free perovskite which helps to replace lead based ceramics which are harmful to environment. Due to its high dielectric constant, low dielectric loss and good tunability, BZT has attracted immense attentions for its potential applications in dynamic random access memory, piezoelectric actuators and microwave technology [5,6].

In recent years, many researchers have studied the effects of sintering temperatures and holding time on the structure and dielectric properties of BZT ceramics [7–15]. It was reported that the maximum of dielectric constant of BZT ceramics increased from 3600 to 5800 as the sintering temperature increased from 1400 to 1550 °C. A further increase in the sintering temperature to 1600 °C results in a drop of the maximum of dielectric constant to 4300 [7]. Mahesh [8] investigated the effect of sintering temperature in the range of 1350–1450 °C on the microstructure and electrical properties of $Ba(Zr_{0.15}Ti_{0.85})O_3$ ceramics, and found that the maximum dielectric constant decreased along with an increase in the degree of diffuseness. However, when the temperature reaches 1450 °C, both the structure and the electric properties deteriorate significantly. So the dielectric constant of BZT ceramics attains the maximum value only at certain temperature, and with further rise in temperature it decreases [9]. Moreover, Cai *et al.* [10] found that when the holding time increases from 0.5 h to 8 h, the average grain size of $Ba(Zr_{0.2}Ti_{0.8})O_3$ ceramics sintered at 1350 °C increases from 25 to 80 μm

*Corresponding author: tel/fax: +86 23 6502 3479,
fax: +86 23 6502 3706, e-mail: *cgyjxy_cqust@163.com*

monotonously. At the same time, the coercive electric field decreases while the remanent polarization increases as the grain size of BZT ceramics increases.

Among the various compositions of BZT, $Ba(Zr_{0.3}Ti_{0.7})O_3$ shows more stable relaxation behaviour, larger tunability and lower dielectric loss. Therefore, $Ba(Zr_{0.3}Ti_{0.7})O_3$ ceramics can be used for tunable application [7,16]. However, the effects of the various sintering temperature and holding time on the structure and electric properties of BZT ceramics have not been analysed systematically together. Therefore, in this paper, we report the effects of sintering temperature and holding time on the microstructure, dielectric properties, ferroelectric properties and piezoelectric properties of $Ba(Zr_{0.3}Ti_{0.7})O_3$ ceramics.

II. Experimental procedure

2.1. Sample preparation

Barium zirconate titanate (BZT) ceramics was prepared by solid state reaction method. The raw materials are barium carbonate (99.8%, AR, Aladdin), titanium dioxide (99.8%, AR, Aladdin), zirconium oxide (99.0%, AR, Aladdin). The starting materials were weighted according to stoichiometry and then mixed and ball milled for 8 h by the planetary ball mill (XQM-4, Tencan powder Co., Ltd, China). After obtained slurry drying, the mixtures were calcined at 1100 °C for 4 h in a chamber furnace (KBF1700, Nanjing Nanda instrument plant, China), and then the calcined powders were ground again for 8 h. After that, the powder mixtures were pressed at 12 MPa into pellets with the size of 10 mm diameter and 1 mm thickness using liquid paraffin as a binder. After liquid paraffin was burnt off, the samples were sintered at 1350 and 1400 °C for 4, 6 and 8 h, respectively. For the measurement of electric properties, the sintered samples were polished and coated with conductive silver paste on the upper and lower surfaces and then burned at 800 °C for 30 min. After that, the samples were poled under DC field of 20 kV/cm for 25 min at 40 °C in a silicone oil bath.

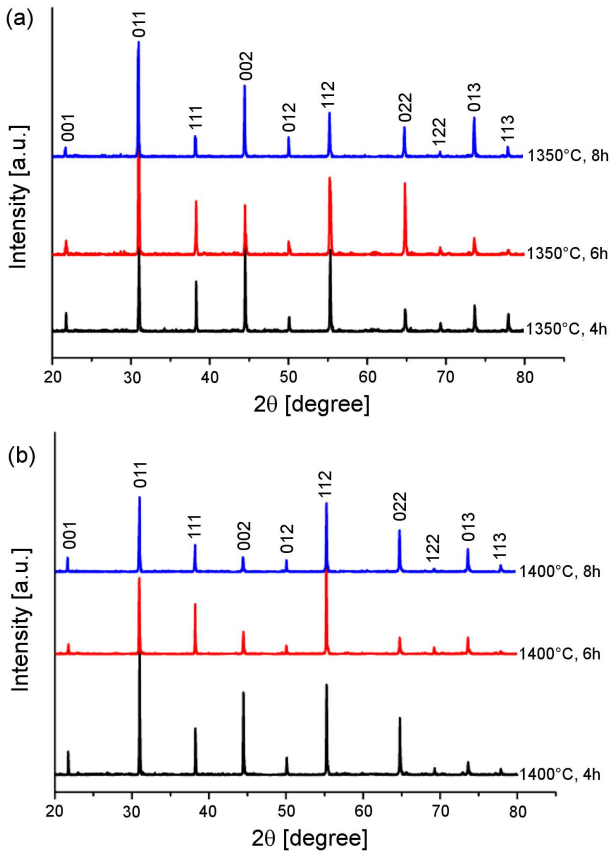

Figure 1. XRD patterns of BZT ceramics sintered at different temperatures: a) 1350 °C and b) 1400 °C

2.2. Samples characterization

The crystalline structure of the BZT ceramics was determined by X-ray diffraction (SmartLab, Rigaku, Japan) using Cu (Kα) radiation source (λ = 1.54178Å) in the 2θ range of 20–80°. The morphologies of the sintered samples were analysed with field emission scanning electron microscopy (S-3700N, Hitachi, Japan). The electric field-induced polarization (*P-E*) and strain (*S-E*) measurements were performed by using a ferroelectric test unit (TF2000, aix-ACCT Inc., Germany), and d_{33} was measured by a quasi-static d_{33} meter (ZJ-4AN, Institute of Acoustics, Chinese Academy of Sciences, China).

The frequency dependence of dielectric permittivity was investigated at room temperature in the frequency range of 20 Hz to 2 MHz by using impedance analyser (E4980A, Agilent, USA). The temperature dependence of the dielectric permittivity was also studied in the temperature range of 0 to 100 °C at 1 kHz. Agilent 4294A was used to characterize the impedance spectroscopy from 100 Hz to 1 MHz at room temperature.

The dielectric constant was calculated from the capacitance using the following equation:

$$\varepsilon_r = \frac{C \cdot t}{\varepsilon_0 \cdot A} \tag{1}$$

where C is the capacitance, d is the thickness of the sample, A is the diameter of the ceramic wafer, and ε_0 is the permittivity of vacuum (8.85×10^{-12} F/m).

The densities (ρ) of BZT ceramics were measured by the Archimedes drainage method, and the porosity of the samples is equal to $(\rho_0 - \rho)/\rho_0$, where ρ_0 is the theoretical density of BZT ceramics [17].

III. Results and discussions

3.1. Crystal structure

The XRD patterns of the BZT ceramics sintered at different temperatures are presented in Fig. 1. It shows that all the BZT ceramic samples have single perovskite phase structure. The absence of any secondary phases proves that the equivalent substitution of Ti^{4+} (0.068 nm) by Zr^{4+} (0.087 nm) results in a homoge-

Table 1. Lattice parameter, relative density and porosity of BZT ceramics sintered at different conditions

Sample	1350 °C/4 h	1350 °C/6 h	1350 °C/8 h	1400 °C/4 h	14000 °C/6 h	1400 °C/8 h
a [nm]	0.43691	0.44425	0.45251	0.44435	0.43220	0.41765
Density [TD%]	94.8	93.7	95.4	94.6	96.3	95.8
Porosity [%]	5.2	6.3	4.6	5.4	3.7	4.2
Grai size [μm]	31.0	33.3	39.6	32.1	34.5	43.4

neous solid solution [11]. In addition, the diffraction peaks of all the ceramics shift towards lower angle, indicating that the lattice parameters are increased due to the substitution by a larger Zr ion at the titanium site (listed in Table 1). Nevertheless, the diffraction peaks of the BZT ceramic samples sintered at 1400 °C shift to higher 2θ angle when the holding time is between 6 and 8 h. This indicates that the larger lattice parameter of the BZT ceramic samples sintered at 1400 °C is achieved at 4 h.

3.2. Surface morphology

Figure 2 shows SEM images of the BZT ceramics sintered at different temperatures. It can be seen that all BZT ceramics shows high density with low porosity and irregularly shaped grains. The relative densities can be used to estimate the density of microstructure of ceramics calculated according to the ratio of the measured density to the theoretical density. The relative densities of the sintered BZT ceramics are in the range from 93.7 to 96.3 %TD, and porosity 3.7 to 6.3% (Table 1). There are some small grains at the boundaries of large grains. This situation is caused by abnormal grain growth [18,19] occurring as a result of very high local rates of interface migration and is enhanced by the topically formed liquid at grain boundaries [9]. Since there is no liquid phase in the SEM images, the abnormal grain growth may have been caused by different mecha-

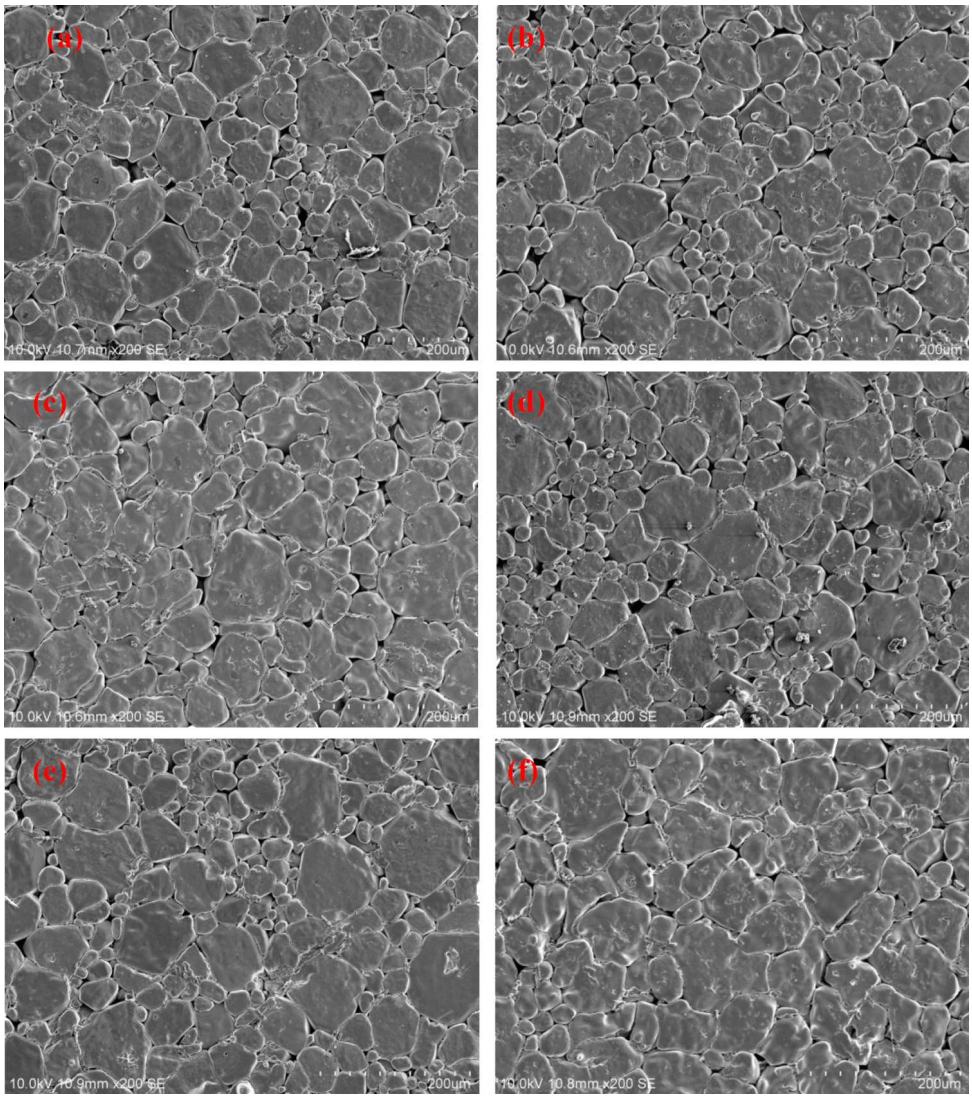

Figure 2. Scanning electron micrograph of BZT ceramics sintered under different conditions: a) 1350 °C/4 h, b) 1350 °C/6 h, c) 1350 °C/8 h, d) 1400 °C/4 h, e) 1400 °C/6 h and f) 1400 °C/8 h

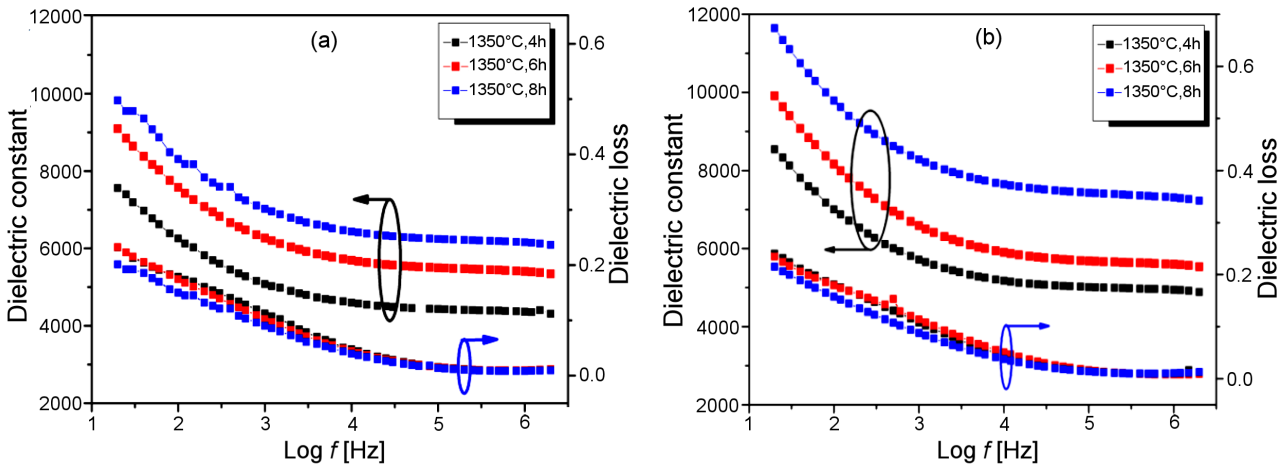

Figure 3. Frequency dependence of the dielectric constant and dielectric loss of BZT ceramics sintered under different conditions: a) 1350 °C and b) 1400 °C

nisms, such as anisotropic grain boundary energies [20].

The average grain sizes of the BZT ceramics were evaluated from SEM images using software Nano Measurer 1.2 and are 31.0, 33.3, 39.6, 32.1, 34.5 and 43.4 μm, for the samples sintered at 1350 °C/4 h, 1350 °C/6 h, 1350 °C/8 h 1400 °C/4 h, 1400 °C/6 h and 1400 °C/8 h, respectively (Table 1). It is obvious that the average grain size of the BZT ceramics increases with the increase of sintering temperature and holding time.

3.3. Dielectric properties

The frequency dependences of ε_r and $\tan\delta$ of the BZT ceramics obtained under different sintering conditions are illustrated in Fig. 3. The following points can be recognised:

1. At low frequencies, the dielectric constant decreases sharply with the increase of frequency, while it tends to be stable at high frequencies. This is due to the different mechanisms of polarization at different frequencies. At low frequency range, the polarization mechanism of ferroelectric materials includes displacement polarization, ion displacement polarization, space charge polarization and dipole transition polarization and all polarization mechanisms contribute to the dielectric constant. At higher frequencies, the dielectric constant may be mainly contributed by the electron displacement polarization mechanism. Many ferroelectric materials have this kind of behaviour [12].
2. The dielectric constant increases with the increase of holding time and sintering temperature, due to the increase of the average grain sizes [13]. The dielectric constant of the BZT ceramics sintered at 1400 °C for 8 h is around 11500.
3. It is observed that the dielectric loss was higher at lower frequencies and that it decreases with the increase of frequency. This is evidence that the sample sintered for 8 h has lower value of loss tangent. With the increase of holding time, the dielectric loss is obviously reduced. It can also be seen (Fig. 3) that the dielectric loss of the BZT ceramics is relatively high. One can conclude that from one hand, as the grain size increases with increased holding time, bigger grain size implies lesser grain boundaries and maybe minor defects and space charges, which will result in lower dielectric loss. On the other hand, the unequal BZT ceramics grain size leads to the anomaly of interaction between grain and grain boundary, thus leading to significant increase in the friction in domain wall motion, therefore dielectric loss of the BZT ceramics is larger [21].

The temperature dependence of dielectric properties for the BZT ceramics at 1 kHz is shown in Fig. 4. It can be seen from Fig. 4a that the maximum dielectric constant of the sample sintered at 1350 °C for 8 h is higher than that of the samples sintered for 4 and 6 h. The maximum dielectric constant of the BZT ceramics sintered at 1350 °C for 8 h at 1 kHz is up to 9000. The maximum dielectric constant of the BZT ceramics sintered at 1400 °C for 6 h is somewhat larger than that of the samples sintered for 4 and 8 h. The maximal dielectric constant of the BZT ceramics sintered at 1400 °C for 6 h at 1 kHz is up to 10500.

In the temperature range from 0 to 100 °C, the temperature dependences of dielectric constant and loss tangent at 1 kHz are shown in Fig. 5. It is interesting that the dielectric peaks slightly shift toward lower temperatures with increasing the sintering temperature. The reason may be that the Zr^{4+} ion (0.087 nm) has a larger ionic size than that of Ti^{4+} ion, and more Zr^{4+} ions can diffuse into the $BaTiO_3$ lattice to substitute Ti^{4+} ions (B site) with increasing the sintering temperature, which can expand the lattice. It also indicates that the maximum dielectric constant of the BZT ceramics sintered 1400 °C is higher than that of the sample sintered at 1350 °C. As seen in Fig. 5a and 5c, the dielectric loss of BZT ceramics sintered at 1400 °C is higher than that of the samples sintered at 1350 °C. While Fig. 5b indicates that near the Curie temperature, the dielectric loss of BZT ceramics sintered at 1350 °C is lower than that

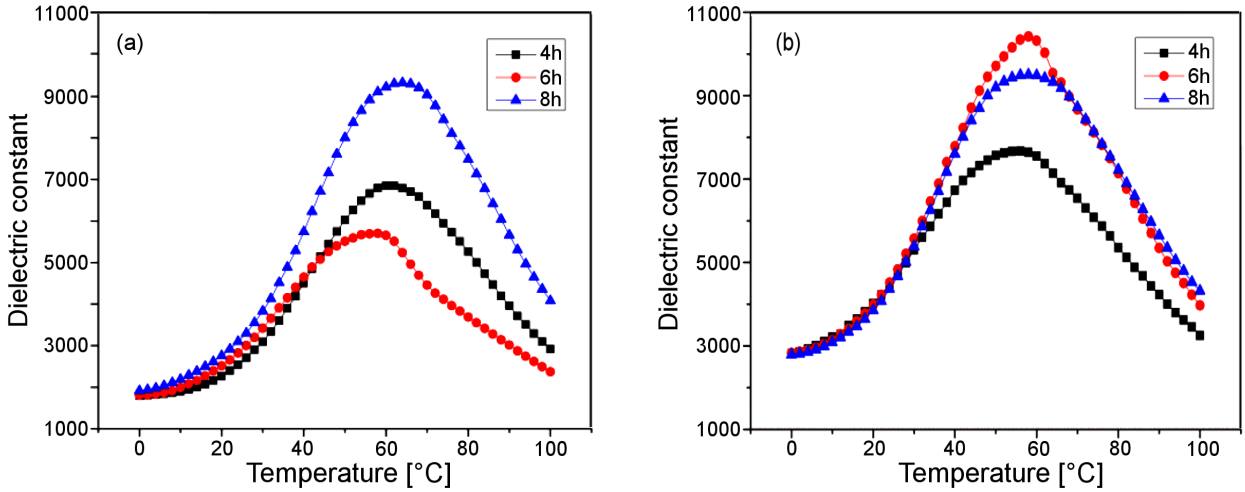

Figure 4. Temperature dependence of the dielectric constant at 1 kHz of the BZT ceramics sintered at various temperatures: a) 1350 °C and b) 1400 °C

of the samples sintered at 1400 °C.

As it is well known, the diffuse phase transition is usually characterized by the deviation from the Curie-Weiss law, and the parameter ΔT_m is introduced to show the degree of this deviation defined as:

$$\Delta T_m = T_{cw} - T_m \tag{2}$$

where T_{cw} indicates the temperature from which the dielectric constant starts to deviate from the Curie-Weiss law, while T_m represents the temperature corresponding to the maximum dielectric constant.

Normal ferroelectrics in the paraelectric state, i.e. above the Curie temperature T_c follow the Curie-Weiss law described by:

$$\frac{1}{\varepsilon} = \frac{T - T_0}{C} \quad (T > T_c) \tag{3}$$

where T_0 is the Curie-Weiss temperature and C is the

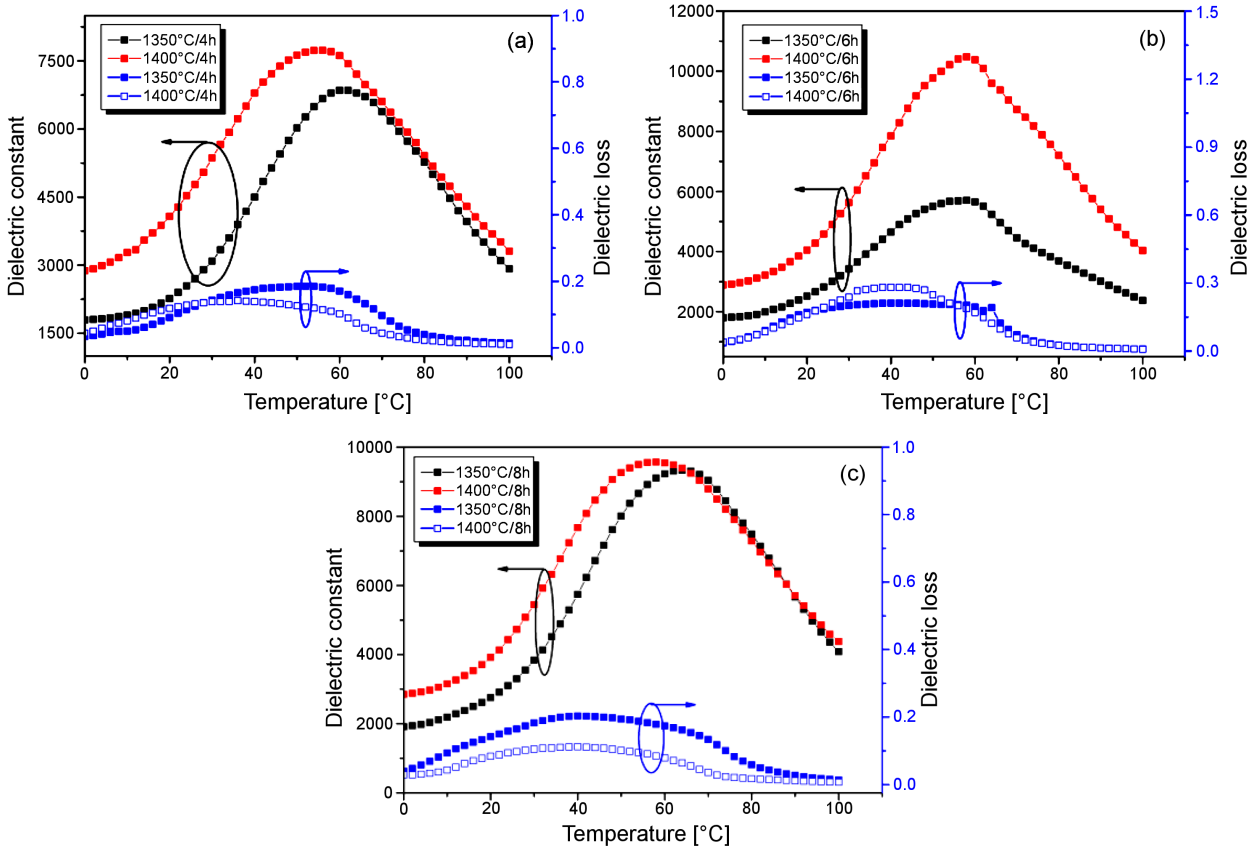

Figure 5. Temperature dependence of the dielectric constant and loss at 1 kHz of the BZT ceramics sintered at various temperatures for: a) 4 h, b) 6 h and c) 8 h

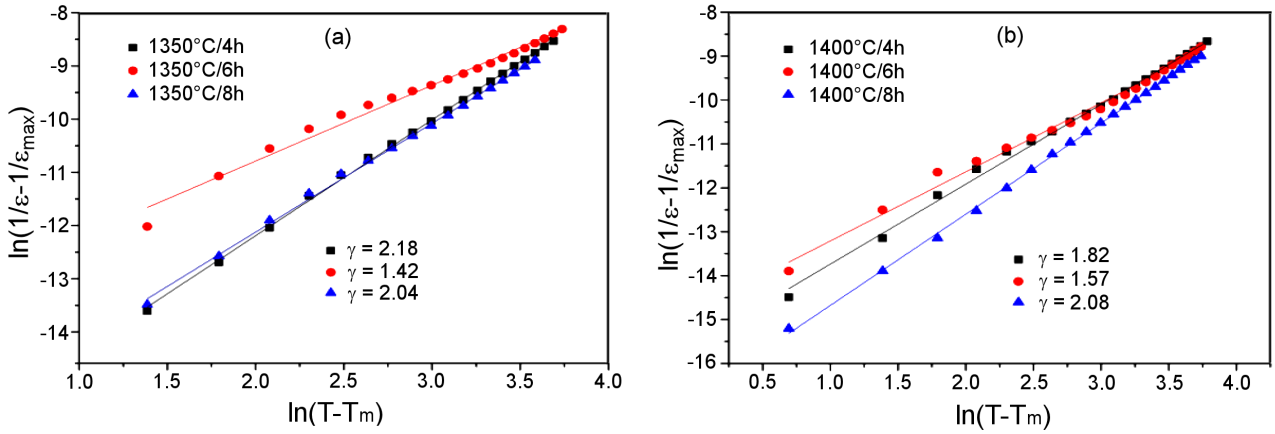

Figure 6. Plots of $\ln(1/\varepsilon - 1/\varepsilon_m)$ as a function of $\ln(T - T_m)$ of BZT ceramic samples: a) 1350 °C and b) 1400 °C

Curie-Weiss constant. A diffuse phase in ferroelectric material is generally characterized by three factors: i) deviation from the Curie-Weiss law in the vicinity of the Curie point, ii) the broadening of the dielectric constant maxima at the Curie temperature and iii) separation between the maximum of dielectric constant and dielectric loss. A modified Curie-Weiss law was proposed by Uchino *et al.* [22] to describe the diffuseness of the ferroelectric phase transition as:

$$\frac{1}{\varepsilon} - \frac{1}{\varepsilon_m} = \frac{(T - T_m)^\gamma}{C'} \tag{4}$$

where γ and C' are assumed to be constants, ε_m represents dielectric constant at T_m and γ is diffuseness constant. The parameter γ gives information on the character of the phase transition: for $\gamma = 1$, a normal Curie-Weiss law is followed, whereas $\gamma = 2$ describes a complete diffuse phase transition.

The plots of $\ln(1/\varepsilon - 1/\varepsilon_m)$ as a function of $\ln(T - T_m)$ for the BZT ceramics sintered at two temperatures are shown in Fig. 6. A linear relationship is observed. The slope of the fitting curves by Eq. 4 is used to determine the γ value (Table 2). Figure 6 shows that the BZT ceramics sintered at high temperature exhibits a strong diffuse phase transition. Probably crystallization was not complete and amorphous phase was present at lower sintering temperature in BZT ceramics, while the crystallization phase with relaxor had been fully formed at higher sintering temperature [14]. However, the diffuseness of phase transition of the BZT ceramics sintered at 1350 °C for 4 h is more than that of the ceramics sintered at 1400 °C for 4 h. The results can possibly be explained as different internal stresses existing in samples with various grain sizes. If the grain size is small, the internal stress can be high, and thus the diffuseness of phase transition enhanced [23].

Figure 7 shows a Nyquist plot (Z' vs. Z'' plot) of all the BZT ceramics studied. Generally speaking, the relation at low test temperatures between Z' and Z'' is linear which gradually converts to semicircle with an increase in the temperature [9]. However, the characteristic semicircles cannot be seen, because of the low test temperatures (≤ 275 °C) the Z'' values are very high indicating high resistivity of the sample and hence the plots obtained at room temperatures linearly line up towards Z'' axis [24].

Table 2. The temperature (T_m) of dielectric constant maximum, the inverse maximum dielectric constant ($1/\varepsilon_m$) and the diffuseness constant (γ) for BZT ceramic samples sintered at different temperatures

Sample	T_m [°C]	$1/\varepsilon_m$ [$\times 10^{-4}$]	γ
1350 °C/4 h	60	1.46	2.18
1350 °C/6 h	58	1.75	1.42
1350 °C/8 h	64	1.07	2.04
1400 °C/4 h	56	1.29	1.82
1400 °C/6 h	58	0.95	1.57
1400 °C/8 h	58	1.05	2.08

The Z'' magnitude of the BZT ceramics for the same holding time decreases with increasing sintering temperature, showing the presence of relaxation process in the material. However, the curves of the samples sintered for 6 h almost coincided. The Z'' values increase as the holding time increases and the impedances of samples sintered for 8 h are the highest (Fig. 7). The reason may be that the porosities of the samples sintered

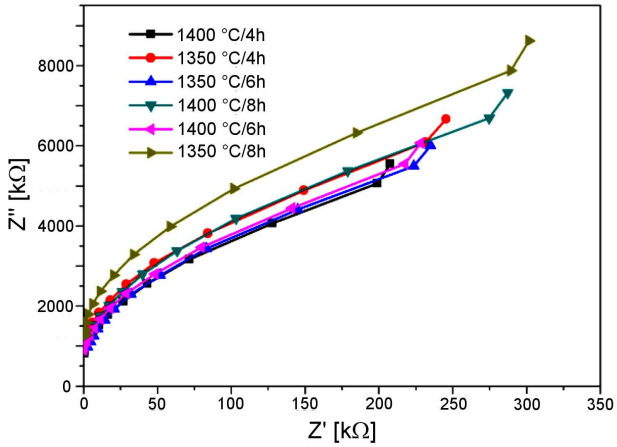

Figure 7. Variation of real (Z') and imaginary part (Z'') of impedance at room temperature for sintered BZT ceramics

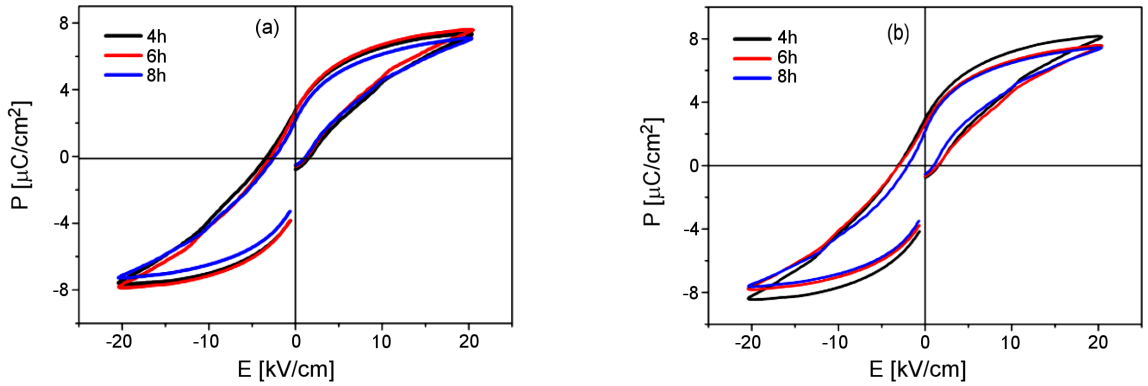

Figure 8. Hysteresis loops of BZT ceramics sintered under different conditions: a) 1350 °C and b) 1400 °C

for 8 h are much lower than in other samples. However, the Z'' values of the samples sintered at 1400 °C for 6 h are lower than that of the samples sintered at 1400 °C for 4 h.

3.4. Ferroelectric properties

Figure 8 shows the ferroelectric hysteresis loops of the BZT ceramics measured at room temperature and 500 Hz. It is seen that all the BZT ceramics have obvious ferroelectric character. The holding time dependences of remnant polarization (P_r) and coercive field (E_c) are shown in Fig. 9. It is found that the remnant polarization and the coercive field of the BZT ceramics sintered at the same temperature decrease as holding time increases except for the sample sintered at 1350 °C for 6 h.

The hysteresis loops of the BZT ceramics can be clearly seen from Fig. 10. The loops were measured by using a triangular voltage pulse with a frequency of 500 Hz at room temperature. As shown in Table 3 and Fig. 10, it can be found that the coercive field of the BZT ceramics sintered for 4 h and 8 h decreases as the sintering temperature increases from 1350 to 1400 °C, which may be due to the size effect. The size of the grains tends to affect the energy barrier required to overcome the domain switching. The larger the grain is, the smaller the energy barrier is required to overcome the domain switching, therefore the smaller coercive field is required.

Figure 10b is the hysteresis loop of the BZT ceramics sintered for 6 h. Although the two curves are almost coincident from the graph, the coercive field increases as the sintering temperature increases according to Table 3. It is also observed that at the same holding time, the remnant polarization of the BZT ceramics sintered for 6 and 8 h decreases as the sintering temperature increases. This result is inconsistent with that reported by Alkathy *et al.* [15]. It is well known that when grains are larger, fraction of grain boundaries is lower. The reversal polarization process of a ferroelectric domain is much easier inside a large grain than in a small grain [6]. Consequently, the remnant polarization enhanced as the grain size increased. However, due to the abnormal growth of grains, grain and grain boundary interaction will be abnormal, which makes the performance of the BZT ceramics to degrade [21]. So the result that shows that the remnant polarization of BZT ceramics decreases as the sintering temperature increases may be abnormal due to the abnormal growth of grains.

Additionally, the hysteresis loops of the BZT ceramics measured at different frequencies are shown in Fig. 11. All ceramics show typical ferroelectric hysteresis loop. It can be seen that the remanent polarization and coercive field decrease with the increase of frequency due to the presence of electron and ion displacement polarization and space charge polarization in the samples. When the frequency increases from 10 Hz to 2 kHz,

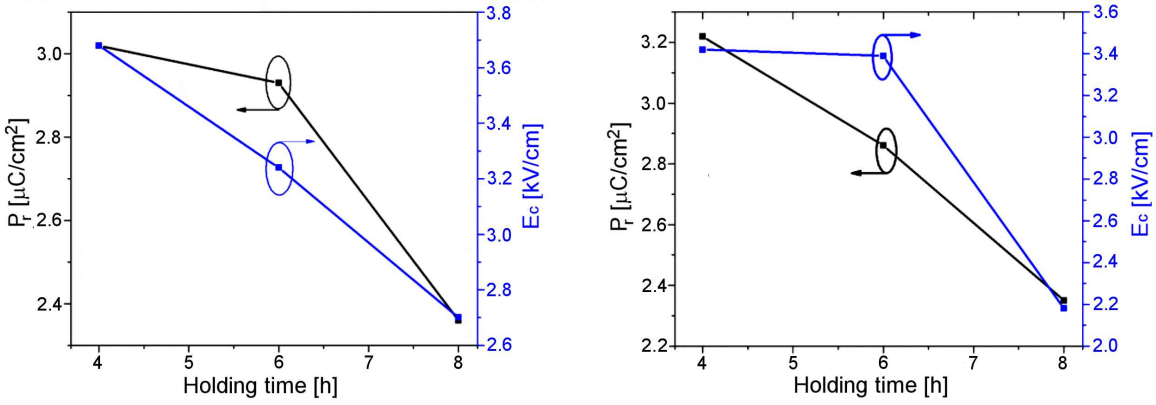

Figure 9. Holding time dependences of the remnant polarization (P_r) and the coercive field (E_c) of the BZT ceramics sintered at: a) 1350 °C and b) 1400 °C

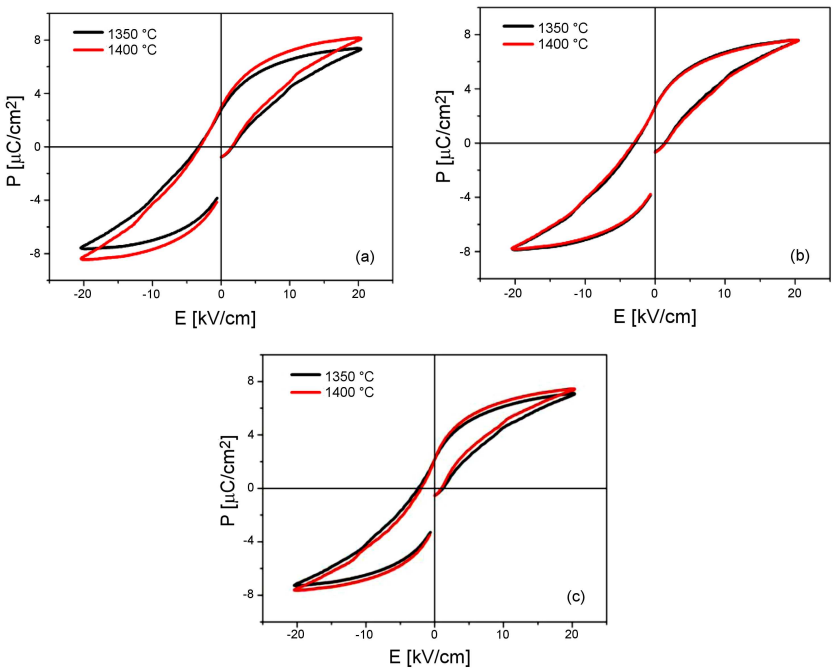

Figure 10. Hysteresis loops of BZT ceramics sintered at different holding times: a) 4 h, b) 6 h and c) 8 h

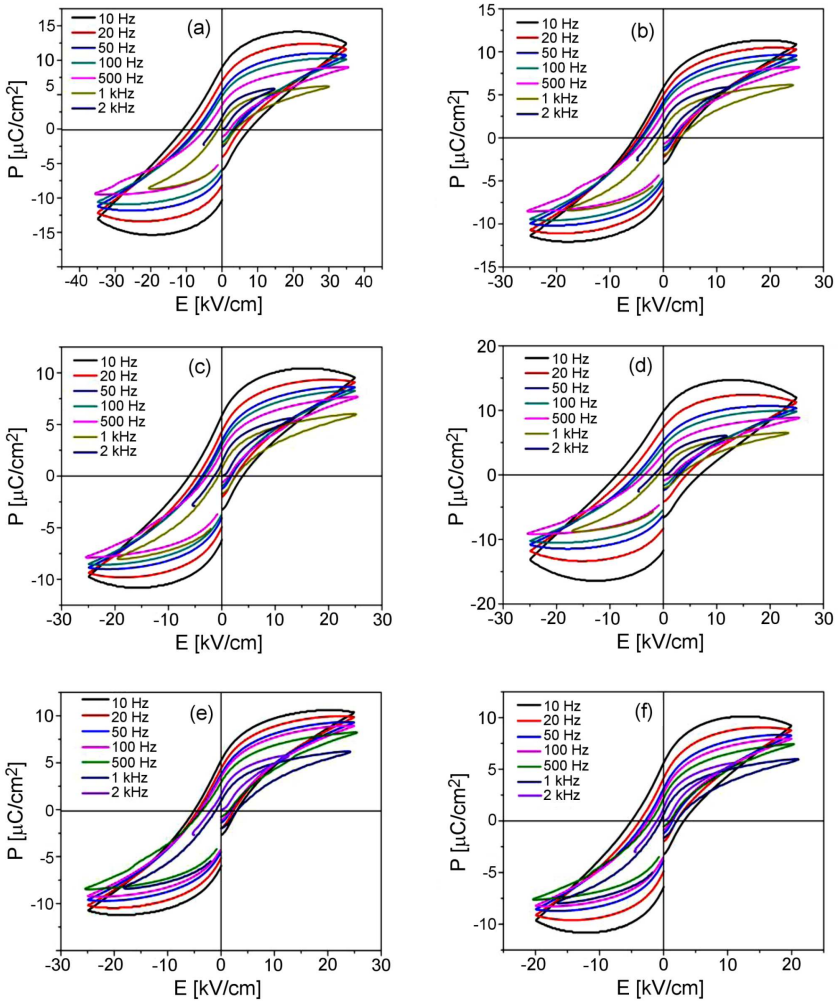

Figure 11. Hysteresis loops at different frequencies of BZT ceramics sintered: a) 1350 °C/4 h, b) 1350 °C/6 h, c) 1350 °C/8 h, d) 1400 °C/4 h, e) 1400 °C/6 h and f) 1400 °C/8 h

Table 3. The coercive electric field (E_c), remnant polarization (P_r) and d_{33} values of sintered BZT ceramics

Sample	Sintering conditions					
	1350 °C/4 h	1350 °C/6 h	1350 °C/8 h	1400 °C/4 h	1400 °C/6 h	1400 °C/8 h
E_c [kV/cm]	3.68	3.42	3.24	3.39	2.70	2.18
P_r [μC/cm^2]	3.02	3.22	2.93	2.86	2.36	2.35
d_{33} [pC/N]	26.8	13.5	35.6	20.9	34	36.7

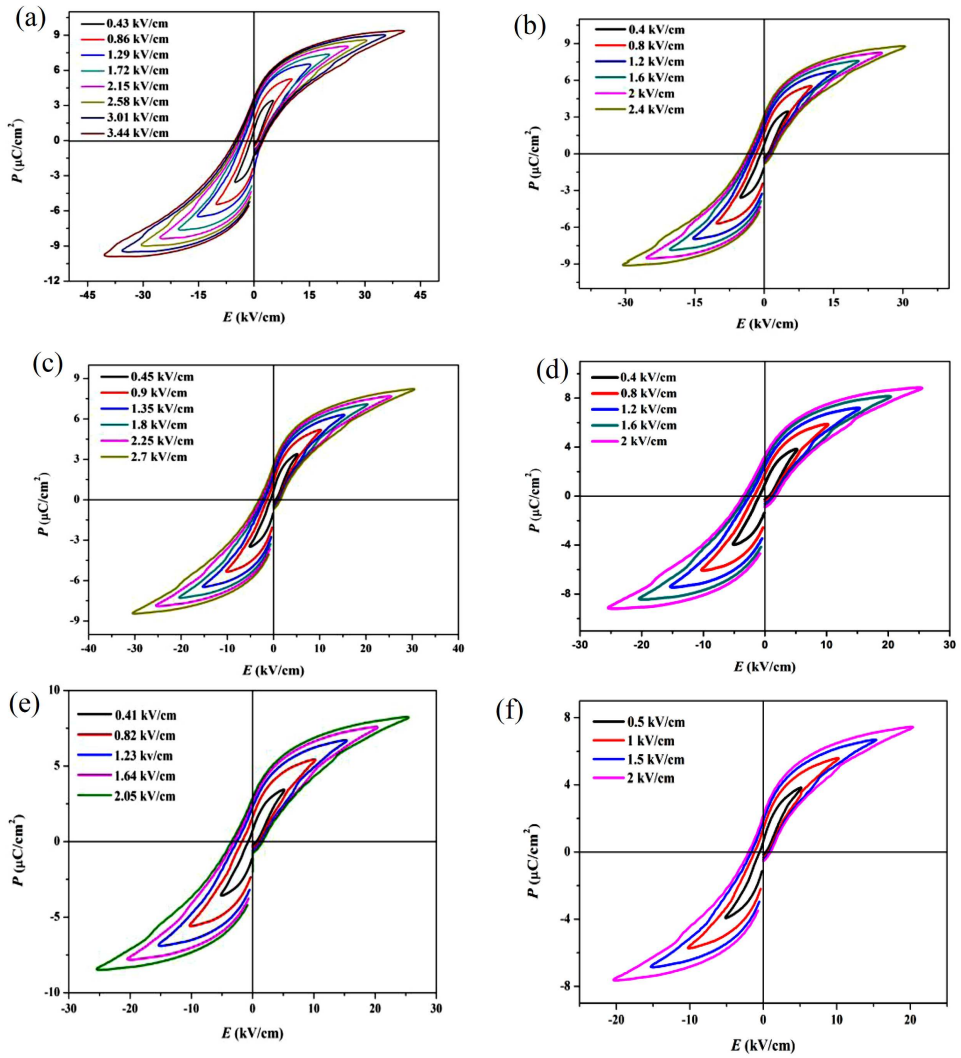

Figure 12. Hysteresis loops of BZT ceramics at different electric field: a) 1350 °C/4 h, b) 1350 °C/6 h, c) 1350 °C/8 h, d) 1400 °C/4 h, e) 1400 °C/6 h and f) 1400 °C/8 h

the space charge polarization cannot keep up with the change of electric field, which leads to the decrease of remnant polarization and coercive field. It can be seen from the Fig. 11 that the hysteresis loops become slender as the sintering temperature and the holding time increase.

Figure 12 shows the room temperature hysteresis loops of the BZT ceramics measured at 500 Hz under different electric fields. It can be seen that the hysteresis loop becomes thinner with the increase of holding time at the same sintering temperature. At the same time, as the applied electric field increases, the electric domain is easier to flip along the external electric field.

Figure 13 shows the bipolar field-induced strain (*S*-*E*) curves for BZT ceramics. The result demonstrates that all samples exhibited a butterfly-shaped strain hysteresis loop with small strain. The strains of the samples sintered at 1350 and 1400 °C for 4 h are larger than that of other samples. The maximum strain (S_{max}) response of 0.023% was obtained for the sample sintered at 1400 °C for 4 h.

3.5. *Piezoelectric properties*

The direct piezoelectric coefficients (d_{33}) of the BZT ceramics measured at room temperature are shown in Fig. 14. The d_{33} values of the BZT ceramics are listed in Table 3. The maximum value is 36.7 pC/N for BZT sample, which was sintered at 1400 °C for 8 h. Hwang

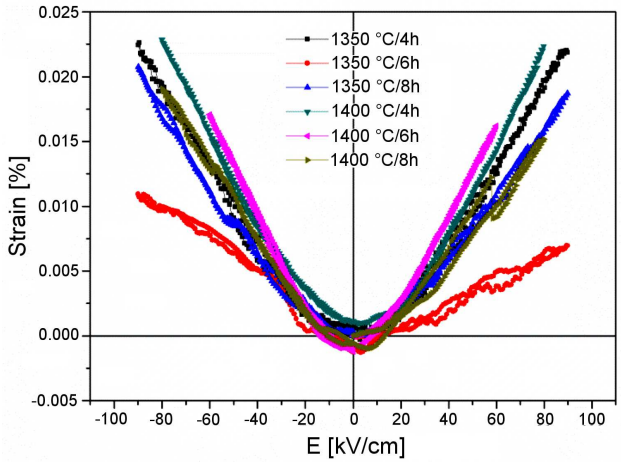

Figure 13. Bipolar *S-E* loops of BZT ceramics

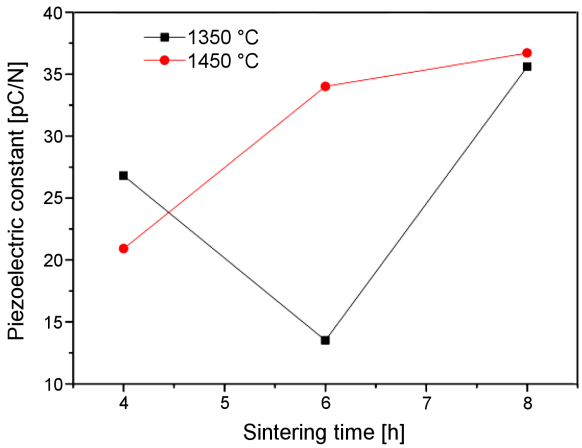

Figure 14. The piezoelectric coefficient (d_{33}) of BZT ceramics

et al. [19] found that the grain size of the piezoelectric ceramics is one of the key factors with a significant influence on the piezoelectric properties. So the uneven grain will greatly affect the piezoelectric properties.

IV. Conclusions

$Ba(Zr_{0.3}Ti_{0.7})O_3$ (BZT) ceramics was prepared by solid state reaction method. In this work, the effects of sintering temperature and holding time on the structure, electrical properties and diffuse phase transition were investigated systematically.

The BZT ceramic samples sintered at 1350 and 1400 °C for 4, 6 and 8 h possess pure perovskite structure. The average grain size of the processed BZT ceramics increases with the increase of sintering temperature and holding time. There are uneven grains in the BZT ceramics sintered at high temperature, which adversely affects the properties of the ceramics. The temperature dependence of the dielectric constant indicates that the diffuse transition behaviour is enhanced with the increase of sintering temperature. The diffuse phase transition behaviour of the BZT ceramics becomes pronounced at a high sintering temperature, implying a sintering temperature-induced diffuse transition. The ferroelectric and piezoelectric properties of the BZT ceramics are directly related to the grain size. The control of the grain size is of great significance to obtain excellent performance of the BZT ceramics.

Acknowledgement: This work was supported by Chongqing Research Program of Basic Research and Frontier Technology (Grant No.CSTC2016jcyjA0175, CSCT2015jcyjA50015), Research Foundation of Education Bureau of Chongqing, China (No.KJ1501310, KJ1501318), National Natural Science Foundation of China (Grant No. 51372283, 51402031, 61404018), the Program for Innovation Teams in University of Chongqing, China (Grant No. CXTDX201601032) and the cooperative project of academician workstation of Chongqing University of Science Technology (Grant No. CKYS201504).

References

1. T. Badapanda, S. Sarangi, B. Behera, P.K. Sahoo, S. Anwar, T.P. Sinha, G.E. Luz Jr., E. Longo, L.S. Cavalcante, "Structural refinement, optical and ferroelectric properties of microcrystalline $Ba(Zr_{0.05}Ti_{0.95})O_3$ perovskite", *Curr. Appl. Phys.*, **14** [5] (2014) 708–715.
2. W. Cai, C.L. Fu, Z.B. Lin, X.L. Deng, "Vanadium doping effects on microstructure and dielectric properties of barium titanate ceramics", *Ceram. Int.*, **37** [8] (2011) 3643–3650.
3. A. Jain, A.K. Panwar, A.K. Jha, "Effect of ZnO doping on structural, dielectric, ferroelectric and piezoelectric properties of $BaZr_{0.1}Ti_{0.9}O_3$ ceramics", *Ceram. Int.*, **43** [2] (2016) 1948–1955.
4. X.G. Tang, Q.X. Liu, J. Wang, H.L.W. Chan, "Electric-field dependence of dielectric properties of sol-gel derived $Ba(Zr_{0.2}Ti_{0.8})O_3$ ceramics", *Appl. Phys. A*, **96** [4] (2009) 945–952.
5. W. Cai, C.L. Fu, J.C. Gao, X.Y. Chen, Q. Zhang, "Microstructure and dielectric properties of barium zirconate titanate ceramics by two methods", *Integr. Ferroelec.*, **113** [1] (2010) 83–94.
6. W. Cai, C.L. Fu, J.C. Gao, X.L. Deng, "Dielectric properties, microstructure and diffuse transition of Ni-doped $Ba(Zr_{0.2}Ti_{0.8})O_3$ ceramics", *J. Mater. Sci.: Mater. Electron.*, **21** [8] (2010) 796–803.
7. T. Bongkarn, P. Nalinee, V. Naratip, "Effect of firing temperatures on phase formation and microstructure of $Ba(Zr_{0.3}Ti_{0.7})O_3$ ceramics prepared via mixed oxide method", *Ferroelectr.*, **383** [1] (2009) 65–72.
8. M.L.V. Mahesh, V.V.B. Prasad, A.R. James, "Effect of sintering temperature on the microstructure and electrical properties of zirconium doped barium titanate ceramics", *J. Mater. Sci.: Mater. Electron.*, **24** [12] (2013) 4684–4692.
9. S. Hajra, S. Sahoo, M. De, P.K. Rout, H.S. Tewari, R.N.P. Choudhary, "Structural and electrical characteristics of barium modified bismuth-sodium titanate $(Bi_{0.49}Na_{0.49}Ba_{0.02})TiO_3$", *J. Mater. Sci.: Mater. Electron.*, **29** [2] (2017) 1463–1472.
10. W. Cai, C.L. Fu, J.C. Gao, H.Q. Chen, "Effects of grain size on domain structure and ferroelectric properties of barium zirconate titanate ceramics", *J. Alloys. Compd.*, **480** [2] (2009) 870–873.

11. W. Cai, J.C. Gao, M.Y. Zhang, C.L. Fu, "Effect of sintering temperature on diffuse phase transition of barium zirconate titanate ceramics", *Integr. Ferroelectr.*, **105** (2009) 1–10.
12. Y. Zhang, H. Sun, W. Chen, "Influence of cobalt and sintering temperature on structure and electrical properties of $Ba(Zr_{0.05}Ti_{0.95})O_3$ ceramics", *Ceram. Int.*, **41** [7] (2015) 8520–8532.
13. X.G. Tang, J. Wang, X.X. Wang, H.L.W. Chan, "Effects of grain size on the dielectric properties and tunabilities of sol-gel derived $Ba(Zr_{0.2}Ti_{0.8})O_3$ ceramics", *Soild State Commun.*, **131** [3-4] (2004) 163–168.
14. Y. Zhang, Y. Li, H. Zhu, Z. Fu, Q. Zhang, "Sintering temperature dependence of dielectric properties and energy-storage properties in $(Ba,Zr)TiO_3$ ceramics", *J. Mater. Sci.: Mater. Electron.*, **28** [1] (2017) 514–518.
15. M.S. Alkathy, R. Gayam, K.C.J. Raju, "Effect of sintering temperature on structural and dielectric properties of Bi and Li co-substituted barium titanate ceramic", *Ceram. Int.*, **42** [14] (2016)15432–15441.
16. S.K. Ghosh, M. Ganguly, S.K. Rout, T.P. Sinha, "Structural and dielectric relaxor properties of A-site deficient samarium-doped $(Ba_{1-2x}Sm_{2x/3})(Zr_{0.3}Ti_{0.7}O_3)$ ceramics", *J. Mater. Sci.*, **49** [15] (2014) 5441–5453.
17. J.T. Tan, Z.R. Li, "Effects of pore sizes on the electrical properties for porous 0.36BS-0.64PT ceramics", *J. Mater. Sci.: Mater. Electron.*, **28** [13] (2017) 9309–9315.
18. G. Han, J. Ryu, C. Ahn, W. Yoon, J. Choi, B.D. Hahn, J.W. Kim, J.H. Choi, D.S. Park, S. Nahm, "High piezoelectric properties of KNN-based thick films with abnormal grain growth", *J. Am. Ceram. Soc.*, **95** [5] (2012) 1489–1492.
19. I. Hwang, D. Do, M.H. Lee, J.K. Da, S.P. Jin, "Effects of forming pressure on the piezoelectric property of lead-free $0.67BiFeO_3$-$0.33BaTiO_3$, ceramics", *J. Korean. Phys. Soc.*, **68** [12] (2016) 1445–1449.
20. A.D. Rollett, D.J. Srolovitz, M.P. Anderson, "Simulation and theory of abnormal grain growth-anisotropic grain boundary energies and mobilities", *Acta. Metal.*, **37** [4] (1989) 1227–1240.
21. S. Sato, Y. Nakano, A. Sato, T. Nomura, "Mechanism of improvement of resistance degradation in Y-doped $BaTiO_3$ based MLCCs with Ni electrodes under highly accelerated life testing", *J. Eur. Ceram. Soc.*, **19** [6-7] (1999) 1061–1065.
22. K. Uchino, S. Nomura, "Critical exponents of the dielectric constants in diffused-phase-transition crystals", *Ferroelectr.*, **44** [1] (1982) 55–61.
23. C.E. Ciomaga, M. Viviani, M.T. Buscaglia, V. Buscaglia, L. Mitoseriu, A. Stancu, P. Nanni, "Preparation and characterization of the $Ba(Zr,Ti)O_3$, ceramics with relaxor properties", *J. Eur. Ceram. Soc.*, **27** [13-15] (2007) 4061–4064.
24. S. Mahajan, D. Haridas, S.T. Ali, N.R. Munirathnam, K. Sreenivas, K. Sreenivas, C. Prakash, "Investigation of conduction and relaxation phenomena in $BaZr_xTi_{1-x}O_3$, (x = 0.05) by impedance spectroscopy", *Physica B*, **451** [451] (2014) 114–119.